A nonsynonymous SNP in the *ITGB3* gene disrupts the conserved membrane-proximal cytoplasmic salt bridge in the $\alpha_{IIb}\beta_3$ integrin and cosegregates dominantly with abnormal proplatelet formation and macrothrombocytopenia

Cedric Ghevaert,[1,2] Alexandre Salsmann,[3] Nicholas A. Watkins,[1,2] Elisabeth Schaffner-Reckinger,[3] Angela Rankin,[1] Stephen F. Garner,[1,2] Jonathan Stephens,[1] Graham A. Smith,[2] Najet Debili,[4] William Vainchenker,[4] Philip G. de Groot,[5] James A. Huntington,[1] Mike Laffan,[6] Nelly Kieffer,[3] and Willem H. Ouwehand[1,2]

[1]Department of Haematology, University of Cambridge, Cambridge, United Kingdom; [2]National Health Service Blood and Transplant, Cambridge, United Kingdom; [3]Laboratoire de Biologie et Physiologie Intégrée, Centre National de la Recherche Scientifique/Research Group-Integrins and Transfer of Information (CNRS/GDRE-ITI), University of Luxembourg, Grand-Duchy of Luxembourg; [4]Inserm U790, Institut Gustave Roussy, Villejuif, France; [5]Department of Haematology, Utrecht Medical Centre, Utrecht, The Netherlands; and [6]Department of Haematology, Imperial College London, London, United Kingdom

We report a 3-generation pedigree with 5 individuals affected with a dominantly inherited macrothrombocytopenia. All 5 carry 2 nonsynonymous mutations resulting in a D723H mutation in the β_3 integrin and a P53L mutation in glycoprotein (GP) Ibα. We show that GPIbα-L53 is phenotypically silent, being also present in 3 unaffected pedigree members and in 7 of 1639 healthy controls. The β_3-H723 causes constitutive, albeit partial, activation of the $\alpha_{IIb}\beta_3$ complex by disruption of the highly conserved cytoplasmic salt bridge with arginine 995 in the α_{IIb} integrin as evidenced by increased PAC-1 but not fibrinogen binding to the patients' resting platelets. This was confirmed in CHO $\alpha_{IIb}\beta_3$-H723 transfectants, which also exhibited increased PAC-1 binding, increased adhesion to von Willebrand factor (VWF) in static conditions and to fibrinogen under shear stress. Crucially, we show that in the presence of fibrinogen, $\alpha_{IIb}\beta_3$-H723, but not wild-type $\alpha_{IIb}\beta_3$, generates a signal that leads to the formation of proplatelet-like protrusions in transfected CHO cells. Abnormal proplatelet formation was confirmed in the propositus's CD34$^+$ stem cell–derived megakaryocytes. We conclude that the constitutive activation of the $\alpha_{IIb}\beta_3$-H723 receptor causes abnormal proplatelet formation, leading to incorrect sizing of platelets and the thrombocytopenia observed in the pedigree. (Blood. 2008;111:3407-3414)

Introduction

Inherited thrombocytopenias are a rare group of diseases with a wide spectrum of clinical phenotypes. Because of their rare occurrence, patients with an inherited low platelet count may be misdiagnosed with autoimmune thrombocytopenia (ITP) and receive inappropriate therapy.[1,2] Among the inherited thrombocytopenias, macrothrombocytopenia constitutes a subgroup in which Bernard-Soulier Syndrome (BSS), caused by mutations in the *GP1BA*, *GP1BB*, and *GP9* genes, is the most common one, with large platelets and severe bleeding.[3] The molecular mechanisms of some of the rarer syndromes which are accompanied by macrothrombocytopenia have also been elucidated. Mutations in the myosin heavy-chain protein (MYH9) were identified in groups of patients with a spectrum of platelet disorders, such as the May-Hegglin anomaly and the Epstein, Fechtner, and Sebastian syndromes.[4,5] The mode of inheritance of these disorders is generally autosomal recessive, but autosomal-dominant forms of a BSS-like disorder caused by nonsynonymous single-nucleotide polymorphisms (nsSNPs) in the *GP1BA* gene have also been reported.[6] More recently, mutations in the transcription factor GATA1 were defined as the cause of X-linked macrothrombocytopenia.[7]

The most frequent autosomal-recessive platelet bleeding disorder is Glanzmann thrombasthenia (GT), which is caused by mutations in the *ITGA2B* or *ITGB3* genes that encode for the integrin $\alpha_{IIb}\beta_3$. This integrin, also named platelet glycoprotein (GP) IIbIIIa, is the most abundantly expressed platelet membrane glycoprotein,[8] and its role is pivotal for platelet function.[9,10] Qualitative and quantitative defects in $\alpha_{IIb}\beta_3$ from patients with GT result in a severe platelet bleeding disorder due to a lack in binding capacity to fibrinogen.[11,12] Typically, patients with GT show absence of platelet aggregation despite a normal platelet count, although some patients with mild thrombocytopenia have been reported.[13,14]

Here, we describe a novel autosomal-dominant platelet disorder with a clinical phenotype consisting of mild thrombocytopenia, platelet anisocytosis, and giant platelets that cosegregates with a nsSNP in the *ITGB3* gene in 5 members spanning 3 generations of a nonconsanguineous pedigree. The mutation, which is absent in healthy controls, replaces the evolutionary highly conserved negatively charged aspartate 3β at position 723 in the cytoplasmic tail of integrin. This residue forms a salt bridge with a IIb, and is crucial for the control of the αarginine residue at position 995 of the lock-open mechanism of $\alpha_{IIb}\beta_3$.[15] Modeling of the consequences of the mutation suggests a disruption of the salt bridge compatible with the findings that platelet $\alpha_{IIb}\beta_3$ in these patients is in a constitutively, albeit partially, activated state. All affected patients also carried a rare nsSNP in the *GPIBA* gene, but further studies in unrelated

Submitted September 20, 2007; accepted November 28, 2007. Prepublished online as *Blood* First Edition paper, December 7, 2007; DOI 10.1182/blood-2007-09-112615.

An Inside *Blood* analysis of this article appears at the front of this issue.

The online version of this article contains a data supplement.

The publication costs of this article were defrayed in part by page charge payment. Therefore, and solely to indicate this fact, this article is hereby marked "advertisement" in accordance with 18 USC section 1734.

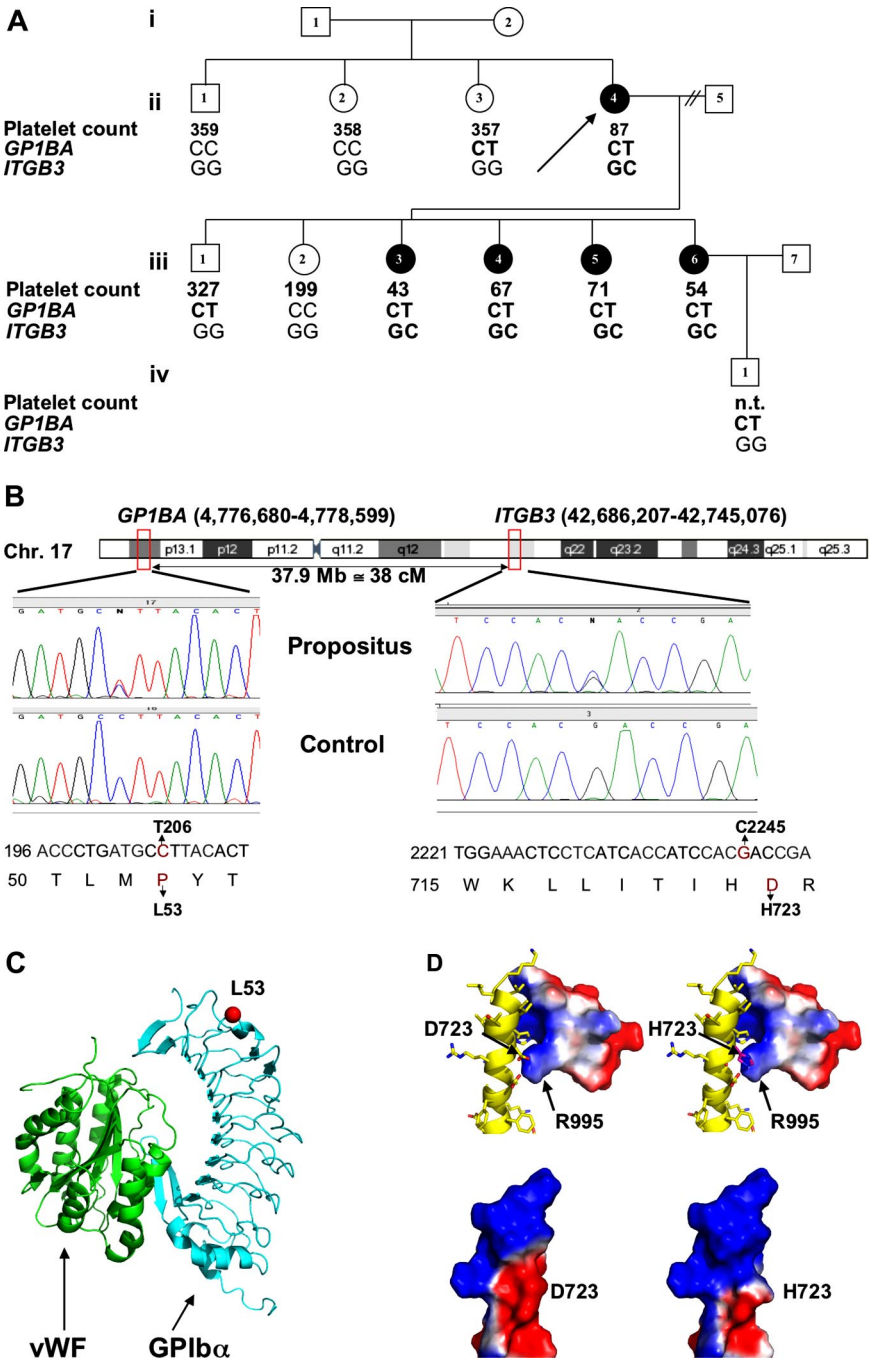

Figure 1. Genetic and structural information and relation with phenotype. (A) Pedigree showing affected (filled) and nonaffected (open) females (circles) and males (squares). The propositus (ii.4) is indicated by an arrow. Platelet counts ($\times 10^9$/L) and the genotypes for the 2 nsSNPs (nucleotide 206 in *GP1BA* and 2245 in *ITGB3*) are given for each member tested (heterozygotes in bold). Where data are lacking, samples were either not available or not tested (n.t.). (B) Top panel shows position of the *GP1BA* and *ITGB3* genes on chromosome 17 (indicated by red boxes). Middle panels show the DNA sequencing traces in the propositus and a control show heterozygous calls (N) at nucleotides 206 and 2245 in the *GP1BA* and *ITGB3* genes, respectively. In the bottom panel, the nucleotides and corresponding amino acids are indicated. The 2 mutations 206C>T and 2245G>C and the amino acid replacements L53P and D723H are presented in red. (C) Ribbon diagram of the VWF (green) and GPIbα (blue) complex based on the crystal structure,[16] which shows residue 53 (red ball) on the convex, non–ligand-facing surface of GPIbα. (D) Modeling of the D723H mutation onto the Nuclear Magnetic Resonance (NMR) structure[17] of the membrane proximal segment of the cytoplasmic tails of α_{IIb} and β_3. top panel show β_3 as a yellow ribbon with side chains showing and a space-filling model of α_{IIb} with the surface colored according to charge, with red indicating negative and blue indicating positive. The overall change in the electrostatic surface potential caused by the D723H mutation is illustrated in the 2 space-filling models of β_3 in the bottom panel with wild-type at the left and mutant at the right showing the loss of negative charge in the mutant. Structural figures were generated using the program Pymol. (DeLano Scientific, Palo Alto, CA).

healthy controls and in pedigree members showed this *GPIBA* mutation to be clinically silent.

Methods

Written informed consent was obtained from all patients in accordance with the Declaration of Helsinki for blood sampling necessary to this study undertaken with the approval of the National Health Service (NHS) Blood and Transplant Institutional Review Board.

Case reports

The propositus is a 49-year-old female (ii.4; Figure 1) who presented with a benign cervical lymphadenopathy. Routine investigations included a blood count, which revealed a reduced platelet count of approximately 80×10^9/L (normal range, 150-350 $\times 10^9$/L) and an increased mean platelet volume (MPV) of 17 fL (normal range, 12-13 fL), both confirmed on repeat testing. A blood film showed marked platelet anisocytosis including giant platelets but no abnormal inclusions (Figure 2A). Clotting screen and plasma fibrinogen levels were normal. She had no bleeding or thrombotic symptoms and was otherwise healthy. A total of 4 of her blood relatives (iii.3, iii.4, iii.5, and iii.6; Figure 1) were subsequently found to have the same platelet abnormality; again, none of them had a bleeding or thrombotic history of note.

Flow cytometry

Platelet membrane GP expression was measured using the following monoclonal antibodies (mAbs): anti-$\alpha_{IIb}\beta_3$ (RFGP56; a kind gift from Prof A. Goodall, University of Leicester, Leicester, United Kingdom); NIBSC-1892110 (National Institute for Biological Standards and Control, Potters

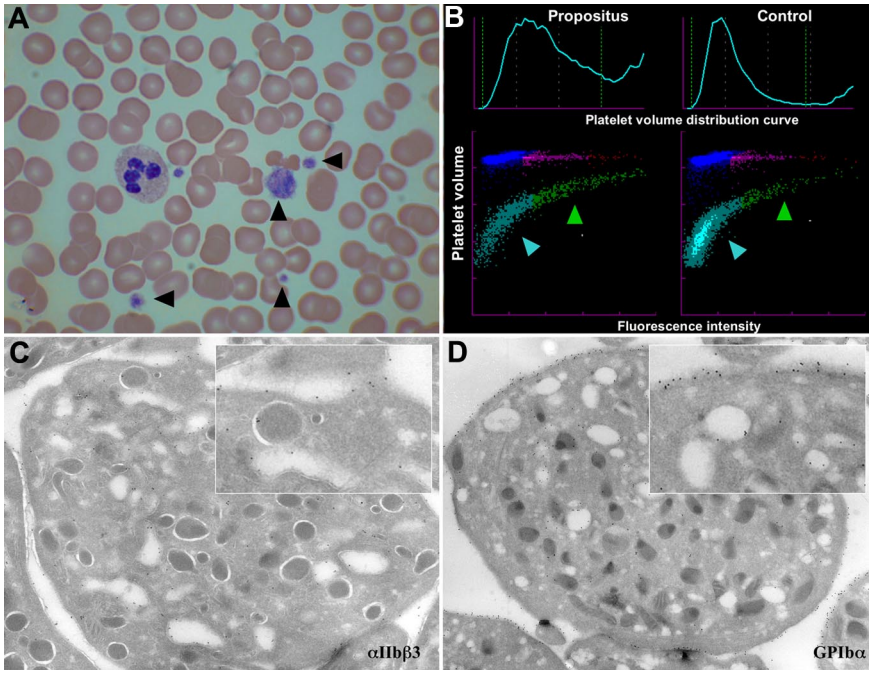

Figure 2. Images of the blood and platelets of the propositus. (A) Light microscopy (×50) of a blood smear with Romanovski stain; platelets are indicated by arrowheads. (B) Flow cytometric scatter plot analysis of platelet RNA content of propositus and control (mean volume as forward scatter and RNA content as fluorescence intensity). The immature platelet fraction is indicated by a green arrowhead, and the mature fraction is indicated by a blue arrowhead. (C,D) Electron micrographs of the propositus's platelets with immunogold staining for $\alpha_{IIb}\beta_3$ (C) and GPIb-IX-V (D). Inserts are a ×7 amplification.

Bar, United Kingdom); CLB-C17 (Sanquin Reagents, Amsterdam, the Netherlands); anti-β3 (Y2/51; Dako, Ely, United Kingdom); anti-GPIbα (CLB-MB45; Sanquin); RFGP37 (a kind gift from Prof A. Goodall); HIP1 (BD Biosciences, Oxford, United Kingdom); AN51 (Dako); anti-GPV (CLB-SW16; Sanquin) and anti-GPIX (FMC25; Serotec, Oxford, United Kingdom); and ALMA.16 (BD Biosciences). Platelets were isolated from EDTA-anticoagulated whole blood, resuspended in phosphate-buffered saline (PBS) containing 10 mM EDTA and 0.25% bovine serum albumin (BSA), and incubated with saturating concentration of mAb; the excess antibody was removed by 3 washes, followed by the addition of FITC-conjugated goat anti–mouse Ig reagent (Dako). Platelet activation markers were analyzed in a whole-blood flow cytometric assay as previously described[18] using FITC-antifibrinogen (Dako), FITC–PAC-1 (BD Biosciences), or PE–anti-CD62P (Sanquin). Data were collected and analyzed using a Beckman Coulter XL-MCL flow cytometer (Beckman Coulter, High Wycombe, United Kingdom).

For CHO cells, $\alpha_{IIb}\beta_3$ expression was assessed with the anti-$\alpha_{IIb}\beta_3$ Pl2-73 (kind gift from Dr Cecile Kaplan, Institut National de la Transfusion Sanguine, Paris, France). For PAC-1 binding experiments, the cells were preincubated in the presence or absence of 1 mM of the inhibitory peptide Arg-Gly-Asp-Ser (RGDS; Sigma, Boornem, Belgium) prior to incubation with PAC-1. Following primary antibody labeling, the cells were washed and further incubated with tetramethylrhodamine isothiocyanate (TRITC)–conjugated goat anti-mouse IgG or IgM (Caltag Laboratories, Burlingame, CA), and flow cytometric analysis was performed on an Epics Elite ESP flow cytometer (Coulter, Hialeah, FL).

Mutation analysis

DNA was extracted from blood samples according to standard methods (Wizard Genomic DNA kit; Promega, Madison, WI). All the exons and flanking introns of the *ITGA2B*, *ITGB3*, *GP1BA*, *GP1BB*, *GP5*, and *GP9* genes were amplified by polymerase chain reaction (PCR) using established methods and sequence analysis performed on an ABI3100 analyzer (Applied Biosystems, Warrington, United Kingdom). After identification of the nsSNPs in the *ITGB3* and *GP1BA* genes, primers and probes were designed to screen 1639 DNA samples from healthy white individuals[19] and other pedigree members by the TaqMan allelic discrimination assay using the Sequence Detection Systems HT 7700 analyser (Applied Biosystems).

Aggregation studies

Platelet-rich plasma (PRP) was isolated from citrated blood samples, and platelet aggregation was assessed using a PAP4 platelet aggregometer (Alpha Labs, Eastleigh, Hants, United Kingdom) after platelet stimulation with ADP (5, 10, and 20 μM), ristocetin (1 and 1.5 mg/mL), arachidonic acid (1 and 1.5 mM), epinephrine (2.5 and 5 μM), or crosslinked collagen-related peptide (CRP-XL; 3, 10, and 20 μg/mL).

Platelet RNA content and thrombopoietin measurement

The immature platelet fraction was determined by a flow cytometric assay on a Sysmex XE 2100 hematology analyzer (Milton Keynes, United Kingdom), as previously described.[20] Plasma thrombopoietin was measured by a standard enzyme-linked immunosorbent assay (ELISA) as published previously.[21]

Electron microscopy

PRP was isolated from 10 mL EDTA-anticoagulated blood and transferred into 4.5 mL of fixative solution (2% paraformaldehyde and 0.2% glutaraldehyde in 0.1 M phosphate buffer [pH 7.4]). After washing, samples were infiltrated with 2.3 M sucrose and frozen in liquid nitrogen. Immunogold labeling was performed on ultrathin cryosection as previously described.[22] After labeling, the samples were washed with distilled water, stained for 5 minutes with uranyloxalate (pH 7.0), and embedded in a mixture of 1.85 methylcellulose and 0.35% uranylacetate at 4°C. Samples were examined using a JEOL 1200 CX electron microscope (Tokyo, Japan).

CHO cells

The cDNA constructs β_3-A723 and β_3-H723 were generated by site-directed mutagenesis (QuikChange XL SDM kit; Stratagene, Amsterdam, the Netherlands), and Chinese hamster ovary (CHO) cells expressing $\alpha_{IIb}\beta_3$-H723 or $\alpha_{IIb}\beta_3$-A723 were generated as previously described.[23]

Megakaryocyte differentiation from CD34$^+$ stem cells

Mononuclear cells were separated over a Ficoll-metrizoate gradient (Lymphoprep; Nycomed Pharma, Oslo, Norway) from peripheral blood. CD34$^+$ cells were then isolated by means of the Miltenyi (Paris, France) immunomagnetic bead technique according to the manufacturer's protocol and grown for 10 days in serum-free Iscove modified Dulbecco medium

(IMDM) supplemented with a combination of pegylated recombinant human megakaryocyte (MK) growth and development factor (10 ng/mL PEG-rHuMGDF; a generous gift from Kirin, Tokyo, Japan) and 50 ng/mL recombinant human stem cell factor (SCF; a generous gift from Amgen, Thousand Oaks, CA).

Adhesion assay

Static adhesion assays were carried out in 96-well microtiter plates or on glass coverslips coated with purified human fibrinogen (Sigma), von Willebrand factor (VWF; kind gift from Dr D. Baruch, Inserm U428, Paris, France), decomplemented fetal calf serum (FCS), or BSA as described.[24] CHO cell transfectants (3×10^4) in 100 μL serum-free IMDM (Gibco, Paisley, Scotland) were preincubated for 30 minutes at room temperature with 10 μM of the $\alpha_v\beta_3$-selective inhibitor RO65–5233/001 (kind gift from Dr S. Reigner, Roche Applied Science, Basel, Switzerland), added to the coated wells, and microphotographed after 2 hours of incubation at 37°C.

Flow studies

Laminar flow studies were performed as previously described[25] using a fibrinogen-coated laminar flow chamber (Glycotech, Gaithersburg, MD) at shear rates of 50, 150, 300, and 600/second for 5 minutes. The number of adherent cells was counted in 4 different 0.8-mm^2 fields using a phase contrast microscope (Axiovert 40 CFL; Zeiss, Jena, Germany).

Immunofluorescence analysis of platelets, proplatelets, and proplatelet-like protrusions

For intracellular immunofluorescence, CHO transfectants, MKs, or platelets were plated onto fibrinogen-coated glass coverslips and fixed for 15 minutes at 4°C in fixation buffer (sucrose 2%, paraformaldehyde 3% in PBS [pH 7.4]). Immunofluorescent staining was performed using the α-tubulin mAb B-512 (Sigma) and TRITC-conjugated phalloidin (Molecular Probes, Leiden, the Netherlands) to visualize tubulin and polymerized actin. The slides were mounted in Mowiol 40–88/DABCO (Sigma) and analyzed with a Leica-DMRB fluorescence microscope (Wetzlar, Germany) using a 63× or a 100× oil-immersion objective. Microphotographs were taken using a Leica DC 300F digital camera and the Leica IM1000 1.20 software. The size of proplatelet swellings were measured on the microphotographs for both control (n = 30) and propositus's proplatelets (n = 15), and the means and standard deviations were calculated.

Results

Platelet glycoprotein expression analysis

In view of the low platelet count and abnormal morphology, we measured the abundance of the fibrinogen and VWF receptors ($\alpha_{IIb}\beta_3$ and GPIb-V-IX, respectively) in the propositus (ii.4) and a further 2 pedigree members (iii.4 and iii.5) by flow cytometry. Increased binding of most antibodies was observed in keeping with the enhanced MPV. However, the reactivity of monoclonal antibodies RFGP37, RFGP56, and Y2/51 against GPIbα, $\alpha_{IIb}\beta_3$, and β_3, respectively, were reduced compared with the control. This suggested an aberrant structure of both GPIb-V-IX and $\alpha_{IIb}\beta_3$ complexes and prompted the sequencing of the exons of the 6 corresponding genes *GP1BA*, *GP1BB*, *GP5*, *GP9*, *ITGA2B*, and *ITGB3*.

Pedigree and population genetic studies

Analysis of the family pedigree (Figure 1A) showed that 4 genes (*ITGA2B*, *GP1BB*, *GP5*, and *GP9*) analyzed were identical to the reference sequence. However, all 5 affected pedigree members carried a 2245G>C nsSNP in exon 14 of the *ITGB3* gene, causing a D723H substitution of the mature β_3 protein and a 206C>T nsSNP in the *GP1BA* gene, introducing a P53L mutation of the mature GPIbα protein (Figure 1B). *ITGB3* and *GP1BA* are both on chromosome 17 at 37.9 Mb apart, giving an approximately 38% chance of crossover per meiosis. Genotyping of 6 additional pedigree members identified individuals ii.3, iii.1, and iv.1, who carried only the *GP1BA* mutation as a result of such a crossover. Further analysis of individuals ii.3 and iii.1 showed normal platelet count, MPV, morphology, and platelet aggregation.

Genotyping of 1639 control DNA samples from healthy donors identified no carriers of the *ITGB3* mutation but identified 7 individuals with the *GP1BA* polymorphism (minor allele frequency [MAF] = 0.0021). Two of them had a full blood count performed, which was normal, and one of these was available for further analysis, which showed normal morphology and aggregation studies.

Platelet ultrastructure and RNA content analysis

Platelet RNA content, a measure of platelet immaturity, was measured in the propositus and patient III.4 and was found to be increased at 19.5% and 26.5%, respectively (normal range, 1.1%-6.1%), with the scatter plot showing that the large platelets were particularly RNA rich, and thus the most immature (Figure 2B). Plasma thrombopoietin levels in the same 2 individuals were normal (not shown). Taken together, these results potentially indicate an increased peripheral platelet turnover. Electron microscopy of the propositus's platelets showed both normal platelet ultrastructure and normal distribution of $\alpha_{IIb}\beta_3$ and GPIb-V-IX (Figure 2C,D).

Modeling of GPIbα-L53 and β_3-H723

We sought to predict the effect of the GPIbα-L53 and β_3-H723 mutations observed in our pedigree on the VWF and fibrinogen receptors by computer modeling. In keeping with the absence of phenotype associated with the GPIbα-L53, residue 53 is located before the first leucine-rich repeat and sits on the convex surface of the horseshoe-shaped GPIbα, on the opposite side to the ligand-binding site (Figure 1C). Modeling of the D723H mutation situated in the membrane proximal cytoplasmic segment of β_3 showed, as expected, a substantial change in the electrostatic surface potential compatible with the disruption of the existing salt bridge between the normally negatively charged aspartate residue at position 723 of β_3 and the positively charged arginine at position 995 of α_{IIb} (Figure 1D).

Platelet function analysis

We investigated the effect of these mutations on platelet function using standard aggregometry methods and flow cytometry. The propositus's platelets aggregated at normal levels after activation with standard agonists (data not shown), but we obtained evidence of spontaneous $\alpha_{IIb}\beta_3$ activation by the binding of the ligand-mimicking antibody PAC-1 to the resting platelets of 2 affected individuals (ii.4 and iii.4) compared with control (11.7% and 10.2% vs 2.5%; Figure 3A). Surface-bound fibrinogen and membrane-expressed P-selectin on resting platelets were both normal, however (Figure 3A), indicating that the β_3-D723H mutation does not cause complete platelet activation. Upon activation with low-, mid- and high-dose ADP and CRP-XL, fibrinogen binding and P-selectin expression reached normal levels when compared with those obtained in 506 healthy individuals[26] (data not shown).

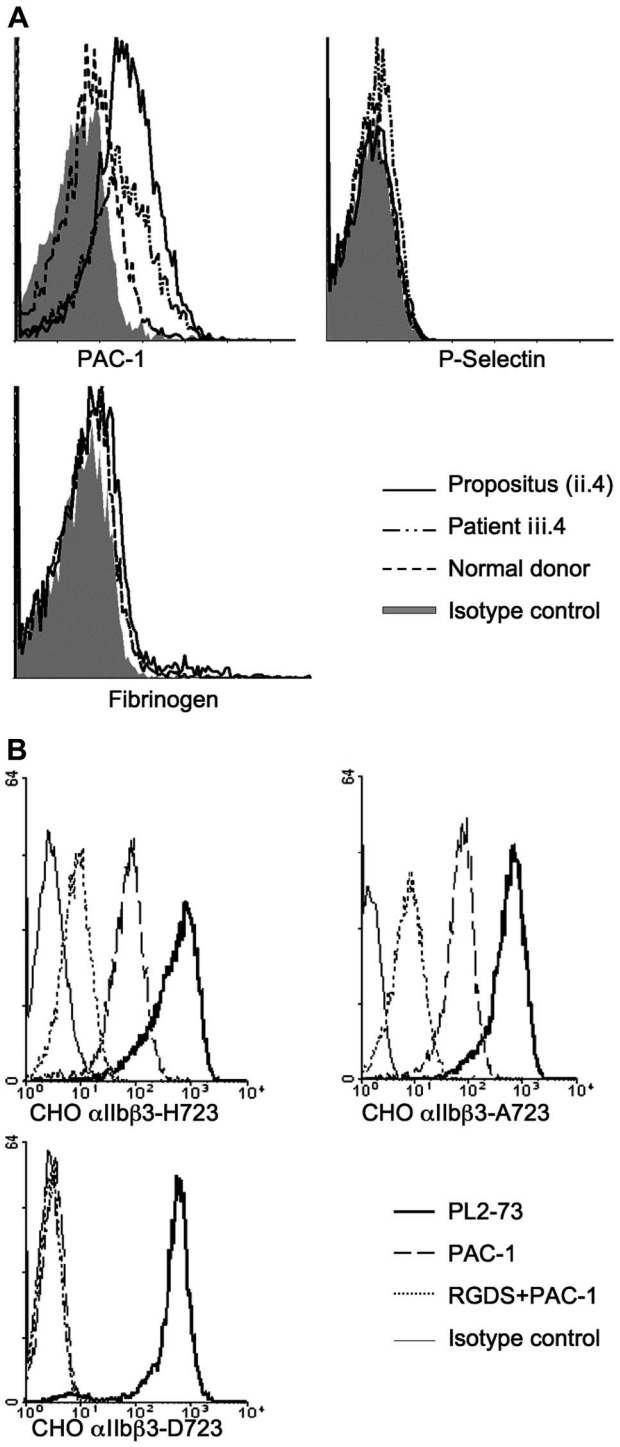

Figure 3. Binding of mAbs measured by flow cytometry to resting platelets and CHO cells transfected with wild-type or mutant $\alpha_{IIb}\beta_3$. (A) Histograms showing increased PAC-1 binding to resting platelets from patients II.4 and III.5 versus control, but no difference of fibrinogen binding or P-selectin surface expression. (B) Histograms showing similar expression levels of $\alpha_{IIb}\beta_3$ (with antibody PL2-73) in all CHO cell lines and increased PAC-1 binding to the $\alpha_{IIb}\beta_3$-H723 and $\alpha_{IIb}\beta_3$-A723 (reversed in the presence of 1 mM RGDS). Irrelevant mouse IgG was used to determine nonspecific antibody binding.

The $\alpha_{IIb}\beta_3$-H723 receptor is constitutively active

To answer the question whether the partial activation of $\alpha_{IIb}\beta_3$ observed with the patients' platelets was caused by the β_3-D723H mutation, we transfected CHO cells with wild-type (WT) $\alpha_{IIb}\beta_3$ and either of 2 mutants $\alpha_{IIb}\beta_3$-H723 or $\alpha_{IIb}\beta_3$-A723. First and as expected, spontaneous and specific PAC-1 binding was observed with $\alpha_{IIb}\beta_3$-H723 and $\alpha_{IIb}\beta_3$-A723 cells, which was not seen with WT cells (Figure 3B). Second, in a static adhesion assay, the $\alpha_{IIb}\beta_3$-H723 cells attached to both fibrinogen and VWF (the latter being dependent upon activated $\alpha_{IIb}\beta_3$[27]), whereas the WT cells only bound to fibrinogen (data not shown). Finally, in laminar flow, $\alpha_{IIb}\beta_3$-H723 cells showed enhanced adhesion to fibrinogen compared with WT cells at all shear rates tested (Figure 4A,B).

Taken together, the results demonstrate that the β_3-H723 mutation causes the constitutive, albeit partial, activation of the $\alpha_{IIb}\beta_3$ complex of the patients' platelets.

CHO $\alpha_{IIb}\beta_3$-H723 cells form proplatelet-like protrusions

We observed that, when plated on fibrinogen, both the $\alpha_{IIb}\beta_3$-H723 and $\alpha_{IIb}\beta_3$-A723 CHO cell lines developed 1 or 2 long protrusions per cell that extended far beyond the original cell boundary (Figure S1, available on the *Blood* website; see the Supplemental Materials link at the top of the online article). These were not observed with WT cells on fibrinogen, nor were they present when the mutant cells were plated on serum proteins, providing evidence that their formation was both driven over the fibrinogen-$\alpha_{IIb}\beta_3$ axis and dependent on the removal of the negatively charged residue at 723. Immunofluorescence staining of the $\alpha_{IIb}\beta_3$-H723 CHO cells showed certain similarities between these protrusions and MK proplatelets: a typical pattern of longitudinally oriented bundled microtubules emerging from the centrosome and extending to the end of the protrusions and continuous actin membrane staining along the protrusions, similar to the actin membrane lining observed in adherent MKs (Figure S1). Furthermore, treatment of mutant cells with nocodazole (a microtubule polymerization inhibitor) abrogated the development of these particular protrusions without interfering with cell adherence (data not shown). These results prompted us to check whether the perturbation of the highly conserved $\alpha_{IIb}\beta_3$ salt bridge interfered with proplatelets formation of in the propositus's MKs.

Abnormal proplatelet formation by the propositus's MKs

We isolated $CD34^+$ stem cells from both the propositus and a healthy control and generated MKs in culture. We observed, in agreement with earlier observations, a substantial increase in the capacity of MKs to develop proplatelets when incubated on fibrinogen, as compared with poly-L-lysine[28] (data not shown), but critically, the proplatelet swellings in the propositus's MKs were significantly increased in size when compared with the control (average $\pm$ SD: 6.8 $\pm$ 0.95 nm vs 4.2 $\pm$ 0.90 nm; $P < .05$; Figure 5). This observation makes it highly likely that the integrin mutation modifies the mechanism of proplatelet formation, leading to the abnormal size and morphology of the platelets.

Discussion

We report here the first patient with a dominantly inherited familial macrothrombocytopenia which cosegregates with a mutation in the *ITGB3* gene. We show that the D723H mutation in the cytoplasmic tail of β_3 is the most likely explanation for the observed phenotype. The replacement of the negatively charged aspartate by histidine perturbs the highly conserved cytoplasmic salt bridge between the α_{IIb} and B_3 intergrin subunits and results in the partial activation of the $\alpha_{IIb}B_3$ complex. This leads to abnormal proplatelet formation and the clinical phenotype.

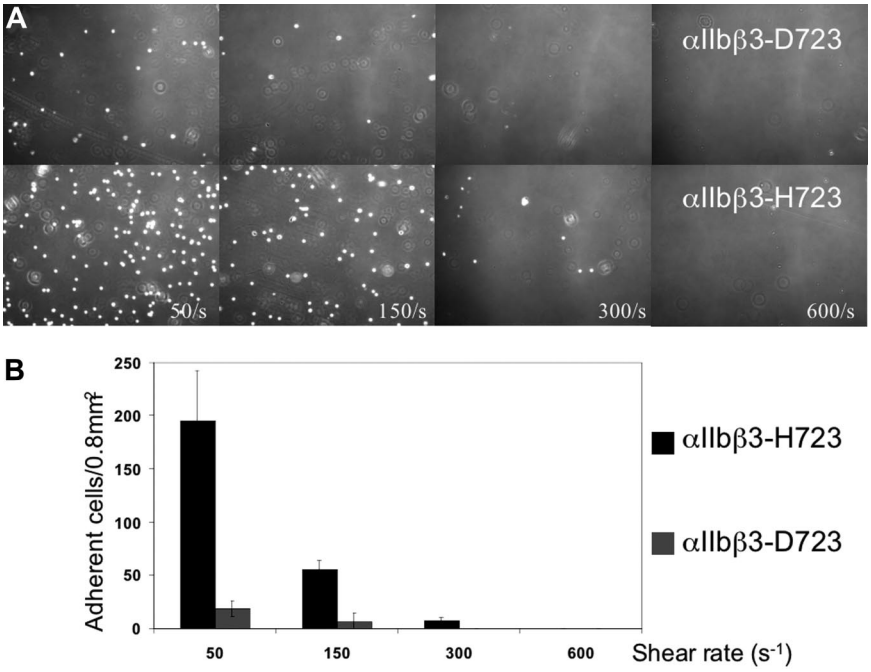

Figure 4. Adhesion of CHO cells to a fibrinogen-coated surface in a laminar flow chamber at different shear rates. (A) Phase-contrast microphotographs of CHO $\alpha_{IIb}\beta_3$-D723 (top panel) and CHO $\alpha_{IIb}\beta_3$-H723 (bottom panel) at shear rates of 50, 150, 300, and 600 s^{-1} (magnification ×20). (B) Quantification of the number of adherent cells in 4 different 0.8-mm^2 fields. Bars represent the means plus or minus 2.5 SD.

In this 3-generation pedigree, 5 β3-D723H mutation–affected individuals were identified who all carried both the and a P53L mutation in GPIbα. We consider it to be highly unlikely that the latter has a clinical and biological relevance for several reasons. First, due to crossover, we identified the GPIbα P53L mutation on its own in 3 further pedigree members, 2 of whom were available for further testing and had normal platelet counts, morphology, and agonist response, including with ristocetin. Second, we also found the *GP1BA* mutation in 7 of 1639 healthy blood donors (MAF = 0.0021), 2 of whom had a platelet count performed that was within normal range. Third, computer modeling showed that residue 53 is situated before the first leucine-rich repeat on the convex face of the horseshoe-shaped domain of GPIbα (Figure 1C), which is not involved in VWF binding. Finally, autosomal-dominant forms of BSS-like syndromes such as the Bolzano variant have been described, but all were associated with mutations in the leucine rich repeats of the molecule (leucine 57 phenylalanine and alanine 156 valine).[29,30] In contrast to our patients, these patients with BSS exhibit a bleeding phenotype and show markedly reduced aggregation to ristocetin. Although we cannot rule out that the β_3 D723H and the GPIbα P53L mutations both need to be present to create the clinical phenotype seen in this pedigree, our findings indicate without doubt that the GPIbα cannot on its own be responsible for the macrothrombocytopenia.

The β_3 D723H mutation was observed in 5 individuals, all affected with macrothrombocytopenia (Figure 1A), and was absent in the 1639 control samples. The negatively charged D723 of the β_3 integrin forms a membrane-proximal cytoplasmic salt bridge with the positively charged R995 in α_{IIb}.[15,30] This salt bridge is evolutionary highly conserved in the integrin family, and its disruption by mutations of either β_3-D723 or α_{IIb}-R995 to alanine shifts CHO cell–expressed $\alpha_{IIb}\beta_3$ from its locked inactive configuration to a constitutively open and active one with increased PAC-1 binding.[15,31] Interestingly, complete activation and fibrinogen binding was only seen when the whole α_{IIb} or β_3 cytoplasmic domains were deleted ($\alpha_{IIb}\Delta 991$ or $\beta_3\Delta 717$).[31,32] In keeping with this concept, prediction by computer modeling of the effect of the histidine at position 723 revealed a similar disruptive effect on the salt bridge (Figure 1D). This was supported by the results of experiments with the patients' platelets and the CHO transfectants. At rest, PAC-1 binding to the platelets was increased, but P-selectin expression and fibrinogen binding were not, indicating that the $\alpha_{IIb}\beta_3$ complex was in a partially activated configuration. The results using CHO cell transfectants confirmed this intermediate activation state of $\alpha_{IIb}\beta_3$-H723 and $\alpha_{IIb}\beta_3$-A723 when compared with the WT complex, with increased PAC-1 but not fibrinogen binding in flow cytometry, increased adhesion to VWF in a static adhesion assay, and increased binding to fibrinogen under shear.

Missense mutations causing activation of the $\alpha_{IIb}\beta_3$ receptor have been previously described in 2 patients with a GT-like phenotype, one with a C560R substitution in the cysteine-rich domain of β_3,[13] and the other with a R995Q substitution in the cytoplasmic tail of α_{IIb}.[14,33] In contrast to our patients, both of these patients presented with overt bleeding symptoms and both showed a greatly reduced (20%) expression of $\alpha_{IIb}\beta_3$ on platelets. Interestingly, the first patient was homozygous for the C560R mutation, and the authors showed that not only PAC-1 binding but also fibrinogen binding to $\alpha_{IIb}\beta_3$ C560R was constitutively increased. The second patient with the α_{IIb} R995Q mutation was compound heterozygous for another, still unknown defect leading to the sole expression of the mutant α_{IIb} R995Q β_3 receptor. In this patient, there was no evidence of increased PAC-1 or fibrinogen binding to resting platelets, but results in transfected cell lines suggested that the α_{IIb} R995Q β_3 receptor was in an intermediate state of activation. The authors showed that the reduced surface expression of the receptor was due to abnormal trafficking of α_{IIb} R995Q β_3 to the surface pool. In our pedigree, the cases are heterozygous for the mutation in the *ITGB3* gene, and the abundance of $\alpha_{IIb}\beta_3$ (50% of which is WT) on the cell surface was in the normal range. Although 2 of the 4 specific monoclonal antibodies used to assess $\alpha_{IIb}\beta_3$ expression on the platelet surface were reduced (RFGP56 and Y2/51), presumably due to a disruption of their epitope by the mutation, the other 2 (NIBSC-1892110 and CLB-C17) fell within normal range.

It would be reasonable to argue that activation of platelet $\alpha_{IIb}\beta_3$ would increase platelet turnover in the circulation, a notion

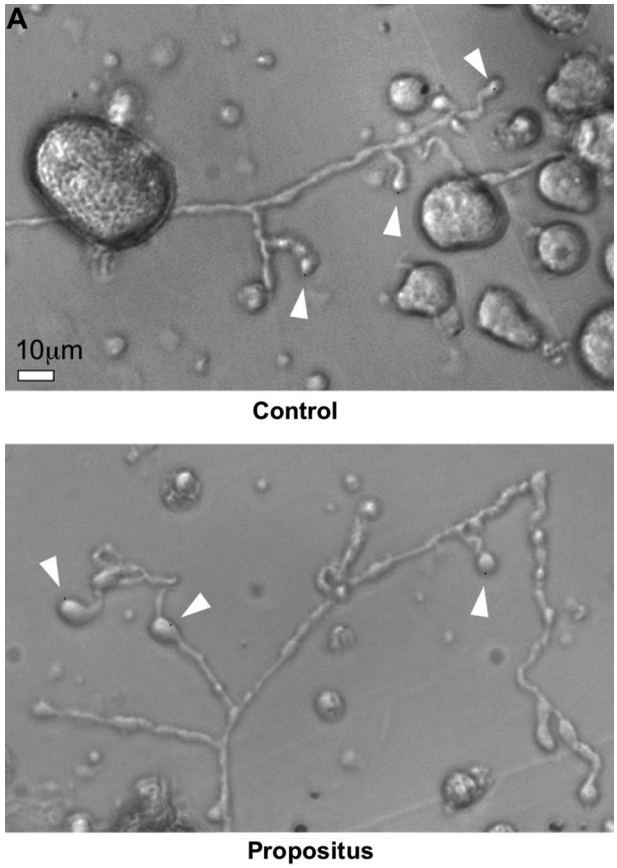

Figure 5. Abnormal proplatelet formation in B_3 D723H megakaryocytes. (A) Light phase-contrast microscopy of propositus and control MKs derived from peripheral blood $CD34^+$ stem cells cultured in serum-free medium for 10 days. Arrowheads point to the proplatelet swellings and the bulbous tips. Scale bar equals 10 μm. (B) Quantification of the average diameter of the proplatelet swellings from propositus (n = 15) and control (n = 30). Bars represent the mean plus or minus SD.

compatible with the patients' thrombocytopenia, the increased platelet RNA content, and the normal plasma thrombopoietin levels. Such a mechanism is observed in patients with platelet-type von Willebrand disease (Pt-VWD) who have a constitutively activated VWF receptor due to an amino acid substitution in GPIbα which enhances binding in the circulation to high-molecular-weight VWF multimers, leading to the consumption of platelets in the periphery.[34] We cannot fully exclude a similar phenomenon in our pedigree, but consider it unlikely for several reasons. First, the grossly abnormal platelet morphology reported here is not seen in patients with Pt-VWD or other disorders associated with increased peripheral platelet consumption such as idiopathic thrombocytopenic purpura (ITP). Second, we did not observe increased in vivo fibrinogen binding to platelets, nor did we observe decreased plasma fibrinogen levels.

A clue to the molecular mechanism explaining the thrombocytopenia and abnormal platelet sizing came from the fortuitous observation that $\alpha_{IIb}\beta_3$-H723 and -A723 CHO cell transfectants spontaneously formed proplatelet-like protrusions when plated on fibrinogen, which were not observed with cells transfected with the WT receptor. Terminally differentiated MKs form platelets by a complex lineage-specific mechanism resulting in the microtubule-driven remodeling of the cytoplasm into long filamentous cell extensions called proplatelets that serve as platelet precursors.[35-37] Proplatelet formation is critically dependent on the chemokine SDF-1 and the growth factor FGF-4, which trigger MK migration from the osteoclast niche to the sinusoid endothelial cells.[38] We and others have shown that outside-in signaling emanating from the interaction of extracellular matrix proteins with MK receptors also controls this process.[39-41] Recent studies in mice have shown that this process is critically dependent on outside-in signaling via $\alpha_{IIb}\beta_3$ after engagement with fibrinogen.[28] We therefore reasoned that the abnormal signal generated by $\alpha_{IIb}\beta_3$-H723, which led to the formation of proplatelet-like protrusions in nonmegakaryocytic mammalian cells would also modify proplatelet formation in the propositus's MKs. Using her $CD34^+$-derived MKs, we showed that there was a significant increase in the size of the terminal proplatelet tips when compared with control, an observation that is compatible with the aberrant platelet size in the peripheral circulation. The overall platelet mass is carefully controlled by a negative regulatory feedback loop via the cMpl-thrombopoietin axis,[42] and this explains, at least in part, the observed mild thrombocytopenia.

In conclusion, we have described a novel mutation in the *ITGB3* gene which leads to the constitutive activation of $\alpha_{IIb}\beta_3$ and causes a dominantly inherited mild thrombocytopenia. The proposed molecular mechanism underlying the phenotype illustrates the importance of the cross-talk between MKs and the bone marrow microenvironment for platelet production and shows how a mutation that modifies the control of integrin activation can lead to defective megakaryopoiesis.

Acknowledgments

We are grateful to the Platelet Immunology Laboratory and in particular to Nicola Caley for her help with the glycoprotein expression flow cytomery assay.

The work was supported by a grant from the National Health Service Blood and Transplant (United Kingdom) and from the University of Luxembourg.

Authorship

Contribution: C.G. coordinated the study, performed the laminar flow assays, and wrote the manuscript; A.S. performed the CHO cell and MK assays; N.A.W. oversaw the molecular aspect of the work and DNA analysis; E.S.-R. performed the CHO cell work, including flow cytometry and adhesion assay; A.R. performed DNA analysis of patients and control population and platelet aggregometry; S.F.G. performed the flow cytometry assays on patients' platelets and CHO cells; J.S. performed the flow cytometry assays on patients platelets and CHO cells; G.A.S. oversaw the glycoprotein expression estimation by flow cytometry; N.D. performed isolation of $CD34^+$ cells from peripheral blood, MK

culture, and proplatelet assay; W.V. oversaw the work on MKs; P.G.d.G. performed the electron microscopy; J.A.H. did the modeling for both mutated proteins; M.L. identified and provided access to the patients; N.K. oversaw the CHO cell work and wrote the manuscript; and W.H.O. oversaw the study and wrote the manuscript.

Conflict-of-interest disclosure: The authors declare no competing financial interests.

Correspondence: Cedric Ghevaert, Department of Haematology, University of Cambridge and National Health Service Blood and Transplant Cambridge, Long Road, Cambridge, CB2 2PT, United Kingdom; e-mail: cg348@cam.ac.uk.

References

1. Najean Y, Lecompte T. Genetic thrombocytopenia with autosomal dominant transmission: a review of 54 cases. Br J Haematol. 1990;74:203-208.
2. Noris P, Spedini P, Belletti S, Magrini U, Balduini CL. Thrombocytopenia, giant platelets, and leukocyte inclusion bodies (May-Hegglin anomaly): clinical and laboratory findings. Am J Med. 1998; 104:355-360.
3. Lopez JA, Andrews RK, Afshar-Kharghan V, Berndt MC. Bernard-Soulier syndrome. Blood. 1998;91:4397-4418.
4. Seri M, Cusano R, Gangarossa S, et al. Mutations in MYH9 result in the May-Hegglin anomaly, and Fechtner and Sebastian syndromes: the May-Heggllin/Fechtner Syndrome Consortium. Nat Genet. 2000;26:103-105.
5. Seri M, Pecci A, di Bari F, et al. MYH9-related disease: May-Hegglin anomaly, Sebastian syndrome, Fechtner syndrome, and Epstein syndrome are not distinct entities but represent a variable expression of a single illness. Medicine (Baltimore). 2003;82:203-215.
6. Savoia A, Balduini CL, Savino M, et al. Autosomal dominant macrothrombocytopenia in Italy is most frequently a type of heterozygous Bernard-Soulier syndrome. Blood. 2001;97:1330-1335.
7. Freson K, Devriendt K, Matthijs G, et al. Platelet characteristics in patients with X-linked macrothrombocytopenia because of a novel GATA1 mutation. Blood. 2001;98:85-92.
8. Wagner CL, Mascelli MA, Neblock DS, et al. Analysis of GPIIb/IIIa receptor number by quantification of 7E3 binding to human platelets. Blood. 1996;88:907-914.
9. Shattil SJ, Kashiwagi H, Pampori N. Integrin signaling: the platelet paradigm. Blood. 1998;91: 2645-2657.
10. Shattil SJ, Newman PJ. Integrins: dynamic scaffolds for adhesion and signaling in platelets. Blood. 2004;104:1606-1615.
11. Nurden AT, Caen JP. Specific roles for platelet surface glycoproteins in platelet function. Nature. 1975;255:720-722.
12. Phillips DR, Agin PP. Platelet membrane defects in Glanzmann's thrombasthenia: evidence for decreased amounts of two major glycoproteins. J Clin Invest. 1977;60:535-545.
13. Ruiz C, Liu CY, Sun QH, et al. A point mutation in the cysteine-rich domain of glycoprotein (GP. IIIa) results in the expression of a GPIIb-IIIa (alphaIIb-beta3) integrin receptor locked in a high-affinity state and a Glanzmann thrombasthenia-like phenotype. Blood. 2001;98:2432-2441.
14. Hardisty R, Pidard D, Cox A, et al. A defect of platelet aggregation associated with an abnormal distribution of glycoprotein IIb-IIIa complexes within the platelet: the cause of a lifelong bleeding disorder. Blood. 1992;80:696-708.
15. Hughes PE, Diaz-Gonzalez F, Leong L, et al. Breaking the integrin hinge: a defined structural constraint regulates integrin signaling. J Biol Chem. 1996;271:6571-6574.
16. Huizinga EG, Tsuji S, Romijn RA, et al. Structures of glycoprotein Ibalpha and its complex with von Willebrand factor A1 domain. Science. 2002;297: 1176-1179.
17. Vinogradova O, Velyvis A, Velyviene A, et al. A structural mechanism of integrin alpha(IIb)beta(3) "inside-out" activation as regulated by its cytoplasmic face. Cell. 2002;110:587-597.
18. Janes SL, Wilson DJ, Chronos N, Goodall AH. Evaluation of whole blood flow cytometric detection of platelet bound fibrinogen on normal subjects and patients with activated platelets. Thromb Haemost. 1993;70:659-666.
19. Watkins NA, O'Connor MN, Rankin A, et al. Definition of novel GP6 polymorphisms and major difference in haplotype frequencies between populations by a combination of in-depth exon resequencing and genotyping with tag single nucleotide polymorphisms. J Thromb Haemost. 2006;4:1197-1205.
20. Briggs C, Kunka S, Hart D, Oguni S, Machin SJ. Assessment of an immature platelet fraction (IPF) in peripheral thrombocytopenia. Br J Haematol. 2004;126:93-99.
21. Folman CC, dem Borne AE, Rensink IH, et al. Sensitive measurement of thrombopoietin by a monoclonal antibody based sandwich enzyme-linked immunosorbent assay. Thromb Haemost. 1997;78:1262-1267.
22. Heynen HF, Lozano MM, de Groot PG, Nieuwenhuis HK, Sixma JJ. Absence of ligands bound to glycoprotein IIB-IIIA on the exposed surface of a thrombus may limit thrombus growth in flowing blood. J Clin Invest. 1994;94:1098-1112.
23. Schaffner-Reckinger E, Gouon V, Melchior C, Plancon S, Kieffer N. Distinct involvement of beta3 integrin cytoplasmic domain tyrosine residues 747 and 759 in integrin-mediated cytoskeletal assembly and phosphotyrosine signaling. J Biol Chem. 1998;273:12623-12632.
24. Salsmann A, Schaffner-Reckinger E, Kabile F, Plancon S, Kieffer N. A new functional role of the fibrinogen RGD motif as the molecular switch that selectively triggers integrin alphaIIbbeta3-dependent RhoA activation during cell spreading. J Biol Chem. 2005;280:33610-33619.
25. Legendre P, Salsmann A, Rayes J, et al. CHO cells expressing the high affinity alpha(IIb)beta3 T562N integrin demonstrate enhanced adhesion under shear. J Thromb Haemost. 2006;4:236-246.
26. Jones CI, Garner SF, Angenent W, et al. Mapping the platelet profile for functional genomic studies and demonstration of the effect size of the GP6 locus. J Thromb Haemost. 2007;5:1756-1765.
27. Kieffer N, Fitzgerald LA, Wolf D, Cheresh DA, Phillips DR. Adhesive properties of the beta 3 integrins: comparison of GP IIb-IIIa and the vitronectin receptor individually expressed in human melanoma cells. J Cell Biol. 1991;113:451-461.
28. Larson MK, Watson SP. Regulation of proplatelet formation and platelet release by integrin alpha IIb beta3. Blood. 2006;108:1509-1514.
29. Ware J, Russell SR, Marchese P et al. Point mutation in a leucine-rich repeat of platelet glycoprotein Ib alpha resulting in the Bernard-Soulier syndrome. J Clin Invest. 1993;92:1213-1220.
30. Miller JL, Lyle VA, Cunningham D. Mutation of leucine-57 to phenylalanine in a platelet glycoprotein Ib alpha leucine tandem repeat occurring in patients with an autosomal dominant variant of Bernard-Soulier disease. Blood. 1992;79:439-446.
31. Hughes PE, O'Toole TE, Ylanne J, Shattil SJ, Ginsberg MH. The conserved membrane-proximal region of an integrin cytoplasmic domain specifies ligand binding affinity. J Biol Chem. 1995;270:12411-12417.
32. O'Toole TE, Mandelman D, Forsyth J, et al. Modulation of the affinity of integrin alpha IIb beta 3 (GPIIb-IIIa) by the cytoplasmic domain of alpha IIb. Science. 1991;254:845-847.
33. Peyruchaud O, Nurden AT, Milet S et al. R to Q amino acid substitution in the GFFKR sequence of the cytoplasmic domain of the integrin IIb subunit in a patient with a Glanzmann's thrombasthenia-like syndrome. Blood. 1998;92: 4178-4187.
34. Miller JL. Platelet-type von Willebrand disease. Thromb Haemost. 1996;75:865-869.
35. Patel SR, Hartwig JH, Italiano JE Jr. The biogenesis of platelets from megakaryocyte proplatelets. J Clin Invest. 2005;115:3348-3354.
36. Italiano JE, Jr., Lecine P, Shivdasani RA, Hartwig JH. Blood platelets are assembled principally at the ends of proplatelet processes produced by differentiated megakaryocytes. J Cell Biol. 1999; 147:1299-1312.
37. Patel SR, Richardson JL, Schulze H, et al. Differential roles of microtubule assembly and sliding in proplatelet formation by megakaryocytes. Blood. 2005;106:4076-4085.
38. Avecilla ST, Hattori K, Heissig B, et al. Chemokine-mediated interaction of hematopoietic progenitors with the bone marrow vascular niche is required for thrombopoiesis. Nat Med. 2004;10: 64-71.
39. Larson MK, Watson SP. A product of their environment: Do megakaryocytes rely on extracellular cues for proplatelet formation? Platelets. 2006;17:435-440.
40. Sabri S, Jandrot-Perrus M, Bertoglio J, et al. Differential regulation of actin stress fiber assembly and proplatelet formation by alpha2beta1 integrin and GPVI in human megakaryocytes. Blood. 2004;104:3117-3125.
41. Nurden P, Debili N, Vainchenker W, et al. Impaired megakaryocytopoiesis in type 2B von Willebrand disease with severe thrombocytopenia. Blood. 2006;108:2587-2595.
42. Kaushansky K. Thrombopoietin: the primary regulator of platelet production. Blood. 1995;86: 419-431.